

Anand S. Patel¹

Department of Radiology and Biomedical Imaging,
University of California San Francisco,
185 Berry Street, Suite 350,
San Francisco, CA 94107-5705
e-mail: anand.patel@ucsf.edu

Maythem Saeed

Department of Radiology and Biomedical Imaging,
University of California San Francisco,
San Francisco, CA 94107

Erin J. Yee

Department of Radiology and Biomedical Imaging,
University of California San Francisco,
San Francisco, CA 94107

Jeffrey Yang

Department of Radiology and Biomedical Imaging,
University of California San Francisco,
San Francisco, CA 94107

Gregory J. Lam

Department of Radiology and Biomedical Imaging,
University of California San Francisco,
San Francisco, CA 94107

Aaron D. Losey

Department of Radiology and Biomedical Imaging,
University of California San Francisco,
San Francisco, CA 94107

Prasheel V. Lillaney

Department of Radiology and Biomedical Imaging,
University of California San Francisco,
San Francisco, CA 94107

Bradford Thorne

Department of Radiology and Biomedical Imaging,
University of California San Francisco,
San Francisco, CA 94107

Albert K. Chin

ChemoFilter, Inc.,
645 Woodstock Road,
Hillsborough, CA 94010

Sheena Malik

ChemoFilter, Inc.,
645 Woodstock Road,
Hillsborough, CA 94010

Mark W. Wilson

Department of Radiology and Biomedical Imaging,
University of California San Francisco,
San Francisco, CA 94107

Xi C. Chen

Materials Sciences Division,
Lawrence Berkeley National Laboratory,
Berkeley, CA 94720

Nitash P. Balsara

Materials Sciences Division,
Lawrence Berkeley National Laboratory,
Berkeley, CA 94720;
Environmental Energy Technologies Division,
Lawrence Berkeley National Laboratory,
Berkeley, CA 94720;
Department of Chemical and
Biomolecular Engineering,
University of California,
Berkeley, CA 94720

Steven W. Hetts

Department of Radiology and Biomedical Imaging,
University of California San Francisco,
San Francisco, CA 94107

Development and Validation of Endovascular Chemotherapy Filter Device for Removing High-Dose Doxorubicin: Preclinical Study

To develop a novel endovascular chemotherapy filter (CF) able to remove excess drug from the blood during intra-arterial chemotherapy delivery (IAC), thus preventing systemic toxicities and thereby enabling higher dose IAC. A flow circuit containing 2.5 mL of ion-exchange resin was constructed. Phosphate-buffered saline (PBS) containing 50 mg doxorubicin (Dox) was placed in the flow model with the hypothesis that doxorubicin would bind rapidly to resin. To simulate IAC, 50 mg of doxorubicin was infused over 10 min into the flow model containing resin. Similar testing was repeated with porcine serum. Doxorubicin concentrations were measured over 60 min and compared to controls (without resin). Single-pass experiments were also performed. Based on these experiments, an 18F CF was constructed with resin in its tip. In a pilot porcine study, the device was deployed under fluoroscopy. A control hepatic doxorubicin IAC model (no CF placed) was developed in another animal. A second CF device was created with a resin membrane and tested in the infrarenal inferior vena cava (IVC) of a swine. In the PBS model, resin bound 76% of doxorubicin in 10 min, and 92% in 30 min ($P < 0.001$). During IAC simulation, 64% of doxorubicin bound in 10 min and 96% in 60 min ($P < 0.001$). On average, 51% of doxorubicin concentration was reduced during each pass in single pass studies. In porcine serum, 52% of doxorubicin bound in 10 min, and 80% in 30 min ($P < 0.05$). CF device placement and administration of IAC were successful in three animals. No clot was present on the resin within the CF following the in vivo study. The infrarenal IVC swine study demonstrated promising results with up to 85% reduction in peak concentration by the CF device. An endovascular CF device was developed and shown feasible in vitro. An in vivo model was established with promising results supporting high-capacity rapid doxorubicin filtration from the blood that can be further evaluated in future studies. [DOI: 10.1115/1.4027444]

Keywords: interventional oncology, medical devices, liver cancer

¹Corresponding author.

Manuscript received November 12, 2013; final manuscript received April 3, 2014; published online August 19, 2014. Assoc. Editor: Rupak K. Banerjee.

Introduction

Hepatocellular carcinoma (HCC), i.e., primary liver cancer) is the third leading cause of death worldwide and has faster mortality than many other cancers [1]. Selective catheter-directed IAC is a standard treatment for HCC confined to the liver but that is not amenable to surgery, which is the situation in up to 75% of new cases worldwide [2,3]. IAC-like approaches such as chemoembolization have demonstrated survival benefits in randomized controlled clinical trials [4] potentially due to improved tumor dose profile. During hepatic IAC, catheters are navigated from the femoral artery into the branch hepatic arteries that feed liver tumors. Embolic and chemotherapeutic agents, such as Dox, are then hand injected slowly into the tumors, approximately over 10 min depending on individual anatomy. Thus IAC leads to an improved tumor dose to systemic toxicity profile compared to intravenous chemotherapy. Nonetheless, previous studies have shown that first-pass hepatic clearance of Dox is between 50% and 70% [5]. Moreover, Dox is known to cause irreversible cardiac failure at cumulative doses above 360 mg, thereby limiting the amount of Dox dose safely deliverable during IAC [6]. Thus, there has been focus on further maximizing local delivery of chemotherapy to targets while minimizing systemic exposure. Clinical [5,7–13] and experimental [14–16] studies demonstrate a positive linear relationship between Dox dose and tumor suppression, providing motivation for delivering high doses of Dox. This is limited due to toxicity; however, since a standard Dox dose (50–75 mg) can cause bone marrow suppression, alopecia, gastrointestinal toxicity, and heart failure [17].

Dox has a high affinity to bind to resin and activated carbons; these substances can be used to eliminate excess Dox in vitro and potentially in vivo [18,19]. Ion-exchange resins are currently used as drug-eluting beads during transarterial chemoembolization (TACE) procedures [20]. Dox is positively charged in vivo at body pH, and therefore can bind to these resins, which contain anionic strong-acid sulfonate groups, similar to chromatography separation used in a wide array of chemical processing. Others have described use of an extracorporeal dialysis-type device in conjunction with high-dose chemotherapy in order to increase tumor response and long-term remission with reduced toxicity [5,9–11,21,22]. However, this extracorporeal approach is technically challenging and has raised safety concerns [23]. Although the approach (Delcath System, New York) is still pending FDA approval, the device leads to blood flow occlusion in the lower half of the body, and diversion of hepatic venous blood to extracorporeal activated carbon filtration chambers during IAC. During this process, chemotherapy is filtered out of the blood via absorption; however, the large chambers can also nonspecifically filter endogenous agents in the blood such as catecholamines. Together, combined with blood flow occlusion in the body, the device can lead to potentially serious hemodynamic disturbances. The device ultimately allows for targeted high-dose organ chemotherapy administration by filtering the residual exiting chemotherapy, but is limited due to its design, safety, expense, and implementation.

The development of a safe, nonocclusive, and high-efficiency intravascular catheter filtration device that could eliminate Dox in the veins draining a targeted organ during IAC, such as the liver, could allow for the use of higher Dox doses during IAC. This would lead to increased tumor dose while still limiting systemic toxicity. Such an intravascular device could be temporarily deployed just prior to the Dox IAC infusion, and left in place for multiple pass binding effects depending on the kinetics of system (ideally no more than 60 min after infusion). The device could then be completely in entirety with no implant left within the patient.

The purpose of this preliminary study was to (1) test in vitro the binding capacity and interaction between resin and Dox; (2) develop a chemotherapy filter using this resin that would allow for delivery of high-dose Dox during IAC; and (3) establish an in vivo experimental model for testing high dose chemotherapy.

Methods of Approach

Our study was divided into 3 phases: (1) in vitro experiments to establish the proof-of-concept that a resin-containing filter can bind Dox from electrolyte solution and pig serum; (2) development of an endovascular CF device prototype using this resin; and (3) in vivo pilot experiments on three swine to establish an animal model and proof-of-concept for future toxicity reduction studies.

In Vitro Studies. A closed-circuit flow model simulating IAC delivery was designed using an ion-exchange resin (Dowex, Sigma-Aldrich, St. Louis, MO). In order to test Dox binding capacity and kinetics of the resin, the model was designed by employing a peristaltic pump (Masterflex, Vernon Hills, IL), with controlled flow rate to match human hepatic blood flow (~750 mL/min) (Fig. 1). Polyvinyl chloride tubing also matched the average human hepatic vein, with the filter segment measuring 1.2 cm in diameter and 6 cm in length [24]. A 1 L PBS solution containing Ca^{2+} and Mg^{2+} was warmed to 37 °C in a glass vessel. The solution simulates physiologic serum electrolyte composition, pH, and temperature. Of note, cations in the blood are theorized to be the primary competitors to Dox binding, which is also cationic at body pH (7.4); however, the model accounts for this by matching serum electrolyte concentrations and molarity (0.150 M).

Within the flow-circuit, a filter column was introduced, filled with resin to a volume matching that of a cone in the hepatic vein (2.5 mL). The resin was immobilized in the circuit by a porous polyethersulfone mesh filter used in dialysis (GVS Filter Technology, Inc., Indianapolis, IN). The pore sizes were 50–200 μm depending on resin particle size as a prior study of carotid embolic protection devices demonstrated these pore sizes allow free passage of blood with acceptable pressure drops [25].

The following experiments were performed in this benchtop flow model:

- (1) “Flow experiment”: 50 mg of Dox (2 mg/mL, Pfizer), a dose similar to that administered in clinical IAC [4], was introduced into the system in 1 L PBS ($n=6$) and allowed to equilibrate over several minutes prior to circulating through the resin binding column.
- (2) “IAC experiment”: 50 mg of Dox (2 mg/mL) was infused slowly over 10 min (simulating clinical IAC) with resin filtration device ($n=6$).
- (3) “Serum experiment”: 50 mg of Dox (2 mg/mL), was introduced into the system in 1 L of porcine serum ($n=6$) and allowed to equilibrate over several minutes prior to contact with the resin. In these experiments, in order to test the binding capacity of resin in a complex physiologic solution, resin was added freely to the 1 L vessel containing the Dox solution.
- (4) “Single pass”: 50 mg of Dox (2 mg/mL) was introduced into the system in 1 L PBS, and allowed to equilibrate over several minutes. The 1 L solution was passed through the resin binding column without any subsequent recirculation of the solution through the resin binding column. A sample was obtained of the subsequent solution. The solution was then passed through the same resin binding column again without any subsequent recirculation, and a sample was taken. This was performed several times to determine first pass effects of the resin without recirculation effects.
- (5) Control experiments were performed for each of the above experiments with the same parameters, but without resin in the system. This was done to ensure binding of Dox to other components of the system, such as glass or tubing, was not significant.

Multiple samples were obtained over time (up to 90 min) from these experiments (or per pass for experimental design #4), and Dox concentrations were measured by UV spectrophotometry at a known wavelength of 480 nm. Dox concentrations (mg/mL) were plotted over time (or per pass for experimental design #4).

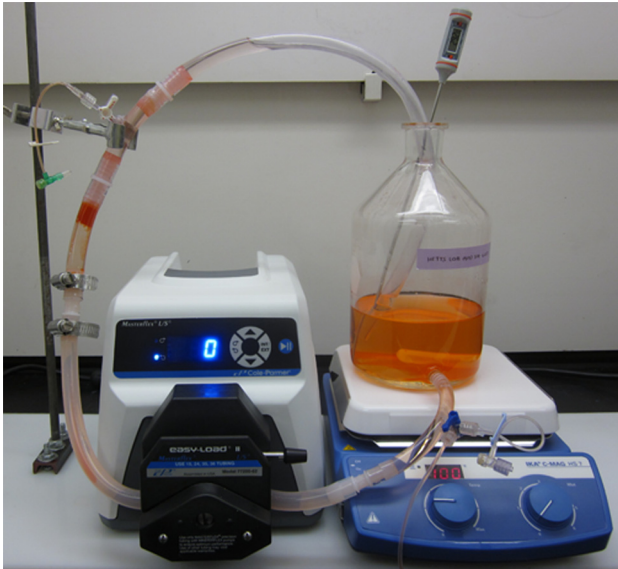


Fig. 1 In vitro flow model simulating TACE. 1 L of 0.05 mg/ml Dox solution was mixed and heated to 37°C. The solution passed via a peristaltic pump through the resin cartridge.

CF Device. Based on these results, an 18 French (F) CF device (CF1) (Fig. 2) was constructed using resin, consisting of extruded plastic tubing for the catheter housing, stainless steel struts supporting a 200 μm nylon mesh dialysis membrane (GVS Filter Technology, Inc., Indianapolis, IN), which immobilized ion-exchange resin beads (approximately 250 μm in diameter) at the catheter tip. The device required an 18F sheath (Cook Medical, Indianapolis, IN) in order to be percutaneously introduced to the target via a jugular vein. Once deployed, the CF1 device morphologically resembled a porous “tea-bag” containing resin beads at the catheter tip. Blood would pass through and contact the resin material allowing Dox to be ionically removed from the blood.

A second 18F CF device (CF2) was constructed with different geometry, resembling a windsock when deployed (Figs. 3(a) and 3(b)). The CF2 device featured an expandable 28 mm diameter Nitinol frame attached to an ion-exchange membrane (UC Berkeley, Professor N. Balsara), which covered part of the

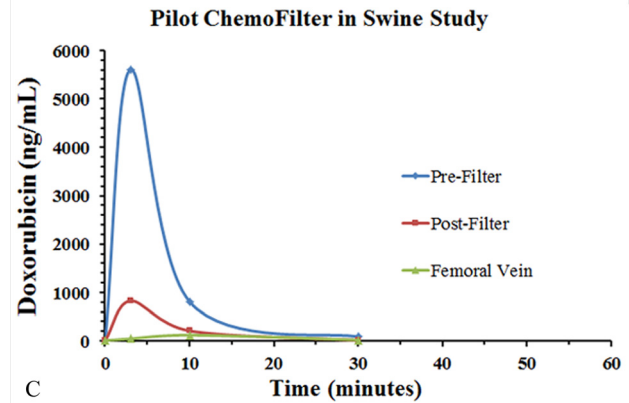
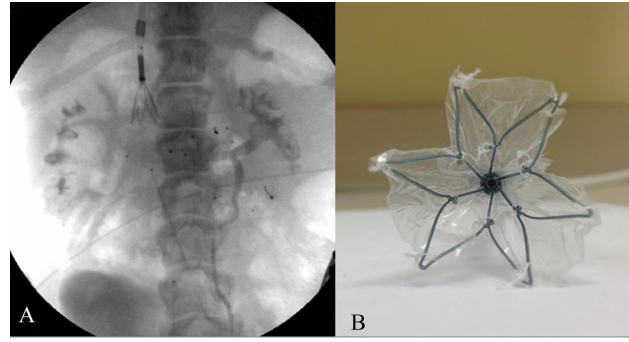


Fig. 3 (a) Fluoroscopic image of the swine demonstrating the CF2 device in place with associated sampling catheters. (b) Photograph of the expanded CF2 device en-face. Notice 22 mm nitinol cage with polymer resin membrane sutured onto the cage. (c) Dox concentration versus time plot with the CF2 device in place during infusion of Dox within the infrarenal IVC. Notice an 85% difference in Dox concentration between prefilter and postfilter samples at 3 min during peak concentration suggesting binding from the CF2 device.

frame. The membrane is a $45 \pm 5 \mu\text{m}$ thick porous film comprising polyethylene (PE) and poly(styrene sulfonate) (PSS) in the form of a PSS-PE-PSS triblock copolymer. The molecular weights of the PE and PSS blocks were 37 kg/mol (46 mol. % sulfonation) and 19 kg/mol. The volume fraction of the pores is 40% and the average pore diameter is estimated to be 12 nm. The pores are

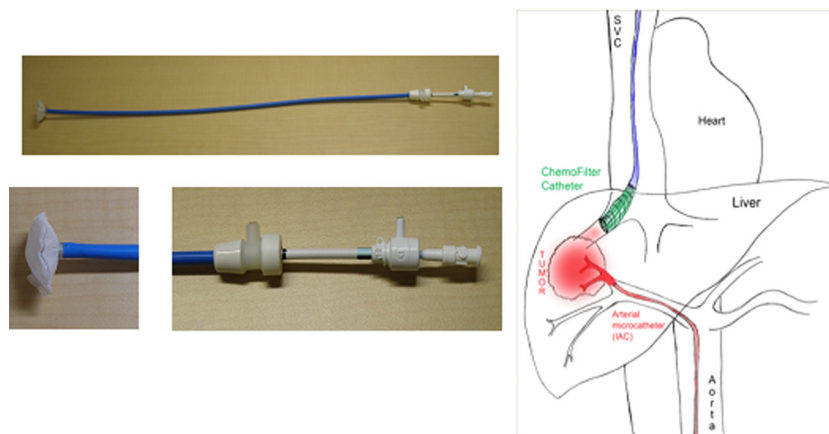


Fig. 2 The CF catheter (left) and schematic illustrating intra-arterial chemotherapy delivery procedure (right). From a percutaneous femoral approach, a microcatheter is guided through the aorta into the arteries feeding a target in the liver to directly infuse Dox. From a percutaneous jugular approach, the CF device is guided through the SVC and deployed in the veins draining the liver.

lined by PSS chains. The center-to-center distance between adjacent pores when the hydrated membrane is 51 nm. Deployment of the device and its mechanism for Dox binding are identical to that described above for the CF1 device.

In Vivo Studies. Farm swine ($n = 3$, 30 kg) received humane care in compliance with the UCSF IACUC. This animal model has similar vascular anatomy and physiology to humans, and has been used extensively in prior IAC simulations [26,27]. Interventional procedures included anesthesia (Isoflurane), X-ray fluoroscopy, percutaneous transarterial catheterization of the hepatic artery, and percutaneous transvenous catheterization of the vena cava. Importantly, heparin was not administered in order to prevent thrombus formation. Heart rate, electrocardiogram, and O_2 -saturation were continuously monitored during the interventions. Animals were euthanized immediately after the procedures.

In the first animal, the CF1 filter was introduced percutaneously via the internal jugular vein (IJV) and deployed in the suprahepatic IVC. Insertion and deployment were assessed in this animal, and no chemotherapy was infused. Venograms were obtained during this procedure via contrast injection (Omnipaque) to assess patency of the venous system. Pressures were measured in the IVC via standard catheter techniques and a digital catheter pressure gauge. At the conclusion of the study, a peripheral blood smear was obtained along with ex vivo analysis of the catheter resin for thrombosis analysis.

In the second animal, a CF device was not deployed, but rather a hepatic artery IAC infusion of Dox was performed with subsequent sampling of blood at various times and positions throughout the venous system. This was performed in order to validate a hepatic Dox IAC pharmacokinetic experimental model, measuring venous Dox concentrations over time via a developed liquid chromatography-mass spectroscopy assay (Pacific Biolabs, Hercules, CA). In this animal, a microcatheter was advanced into the hepatic artery via standard access from a right femoral artery approach using fluoroscopy and contrast as needed. Via percutaneous IJV access, central catheters were positioned with tips in the suprahepatic IVC and right hepatic vein. Next, 50 mg of Dox (2 mg/mL) was administered into the liver via an infusion pump at a constant rate over 10 min. Blood samples were obtained for Dox concentration measurements from each of the 3 above-described central and peripheral venous catheters, at times 0, 3, 10, 30, 60, and 90 min.

In the third animal, under X-ray fluoroscopy and contrast venography, the CF2 device was percutaneously introduced via the internal jugular vein and deployed in the porcine infrarenal IVC. In order to demonstrate binding in vivo solely from the blood, without effects from the liver, 50 mg of Dox (2 mg/ml) was injected over 10 min in the IVC below the CF2 device. Venous catheters with tips proximal and distal to the CF2 device in the infrarenal IVC obtained pressures and blood samples for Dox concentrations over 90 min across the device (Fig. 4).

Statistical Analysis

Dox binding capabilities of resin in the flow and IAC experiments were analyzed and compared to results from control experiments without resin. Statistical differences were explored using an unpaired Welch's t -test. All tests were one-sided and a converted P value of less than 0.05 was considered statistically significant. In the experiments, the t -test was conducted at each time point and analyzed compared to the control. The results indicate a 99.9% confidence interval for the "Flow experiments" and "IAC experiments" and a 95% confidence interval for the "Serum experiments". This statistical power reinforces the significance of resin binding capabilities.

Results

The binding capacity and kinetics of resin were explored via several bench-top experimental designs. In the "Flow experiments" with Dox initially equilibrated in PBS, the resin

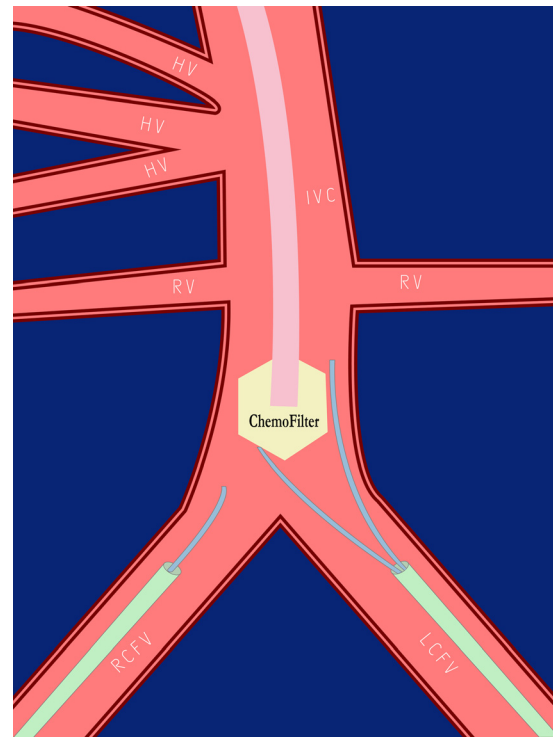


Fig. 4 Schematic of in vivo swine experiment with the CF2 device. The device was placed in the infrarenal IVC (below the RV and HV) from a jugular vein approach. Via access from the RCFV and LCFV, prefilter and postfilter sampling catheters were placed. A Dox infusion catheter was placed inferior to this. This configuration allows for determination of potential concentration drops due to the CF2 device.

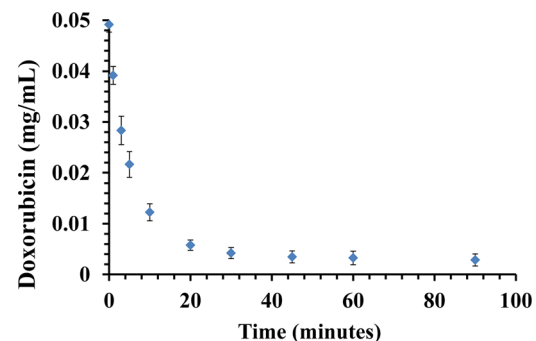


Fig. 5 Flow experiment. A plot shows Dox (0.05 mg/ml) clearance from PBS over the course of 90 min in the flow model. The maximum clearance was 92% and reached at 30 min, suggesting that resin has been saturated. Data are presented as a mean \pm SD, $n = 6$.

bound 76% (38 mg) of Dox (50 mg) within the first 10 min, and 92% (46 mg) within the first 30 min ($P < 0.001$), compared to control experiments with no resin where Dox concentrations remained unchanged over time (Fig. 5). Moreover, in the "IAC experiments" in which Dox was infused slowly over 10 min, the resin filtered 64% (32 mg) of the injected Dox (50 mg) within the first 10 min compared to controls (Fig. 6). At 30 and 60 min, 92% (46 mg) and 96% (98 mg) of Dox was cleared, respectively ($P < 0.001$).

Using the same resin, porcine "Serum experiments" revealed slightly slower kinetics and binding capacity compared to binding from Dox in PBS solution with approximately 52% (26 mg) of

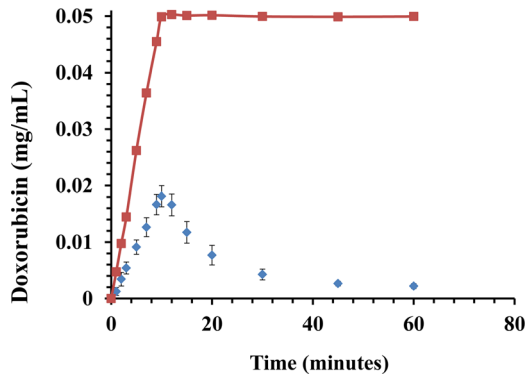


Fig. 6 IAC experiment. A plot shows Dox clearance over the course of 60 min. A dose of 50 mg Dox (0.05 mg/mL) was infused over the course of 10 min with (diamonds) and without filter (squares). Note the high rate of Dox binding to resin during infusion. Data are presented as a mean \pm SD, $n = 6$.

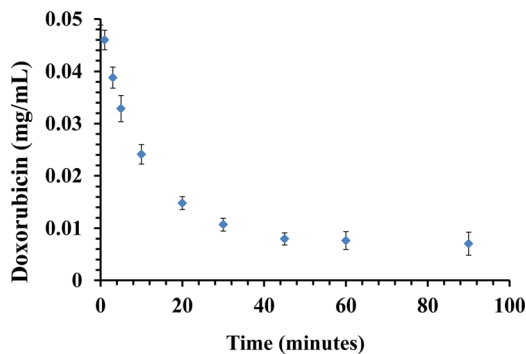


Fig. 7 Serum experiment. A plot shows Dox (0.05 mg/mL) clearance from porcine serum over the course of 90 min. The maximum clearance was 84% at 45 min. Data are presented as a mean \pm SD, $n = 6$.

total Dox mass bound (50 mg) after 10 min and 80% (40 mg) of total Dox mass bound after 30 min ($P < 0.05$) (Fig. 7).

“Single pass” experiments were performed to investigate effects on Dox binding without recirculation of the Dox solution through the resin column. A total of 6 passes were performed with starting Dox concentration of 0.05 mg/ml, and final concentration of 0.0006 mg/ml. On average, Dox concentration was reduced exponentially by 51% compared to each subsequent pass through the resin column (Fig. 8). A total of 99% of the initial total drug mass was bound by the resin after 6 passes.

In vivo, in the first swine, the 18F CF1 device was successfully inserted and deployed with resin contained within the tip of the catheter. Venography after 20 min of deployment, however, demonstrated a focal occlusion of the IVC adjacent to the tip of the catheter (Fig. 9). The bag at the tip of the catheter was packed too densely with the resin beads, causing mechanical venous obstruction. This was also manifested by IVC pressure gradients ranging from 20–30 mmHg, well above the baseline of 5–10 mmHg. Despite IVC occlusion, hemodynamic changes in the swine were minimal, likely due to collateral blood flow in the azygos system. The catheter was removed and the resin bag was examined ex vivo microscopically, revealing no evidence of thrombosis within the resin itself (Fig. 10). This suggests that the occlusion was outside of the catheter and due to obstruction of flow by the resin-containing bag, rather than by the resin itself. Indeed, the cation exchange resin contains highly sulfated groups that are similar to those found in heparin, aiding in biocompatibility and lowering thrombogenicity.

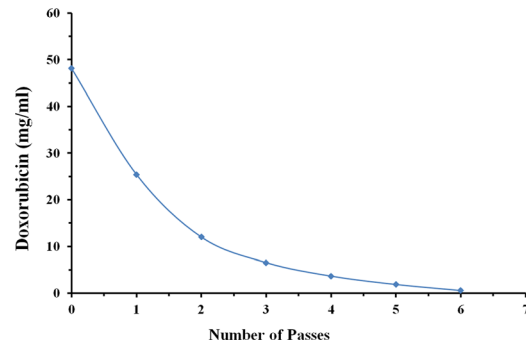


Fig. 8 Single-pass experiment. The plot demonstrates that Dox concentration was reduced from 0.05 mg/ml to 0.0006 mg/ml (99% of initial drug mass reduced) after 6 single passes through the resin column without recirculation of solution. On average, Dox concentration was lowered by 51% during each pass.

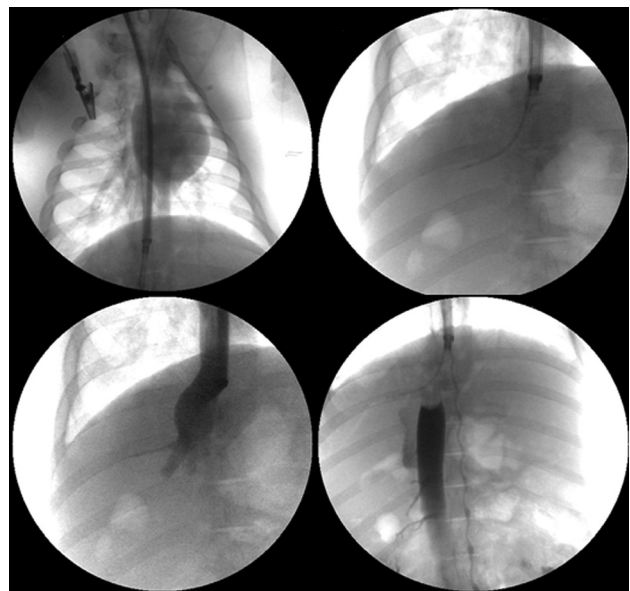


Fig. 9 X-ray fluoroscopy demonstrates the establishment of the in vivo swine model. Top left image demonstrates introduction of device (18 French) through right jugular vein into the suprahepatic IVC. Top right image demonstrates the device tip in the suprahepatic IVC with guide wire securing access into the right hepatic vein. Bottom left image demonstrates a venogram through the device and the patency of hepatic veins and supra-hepatic IVC. Bottom right, a venogram demonstrates a filling defect in the suprahepatic IVC just inferior to the catheter tip after resin introduction into the catheter tip. Collateral flow to the heart is visualized through the azygos venous system.

In the second swine, Dox was successfully administered via hepatic IAC. Assayed Dox concentrations were plotted over time and consistent with prior studies [8,28], thus establishing an in vivo large animal model for further testing of a CF device with hepatic IAC. There were no hemodynamic changes during the procedure.

In the third swine, the CF2 device was successfully introduced and deployed in the infrarenal IVC. Visualization under X-ray fluoroscopy verified the proper placement and mechanical expansion of the Nitinol framework. Pressure measurements taken throughout the experiment yielded a max gradient of 17 mmHg across the CF2 membrane. There were no hemodynamic instabilities based on vital signs. Venography demonstrated non-flow-limiting thrombus below the CF2 device after 90 min of deployment.

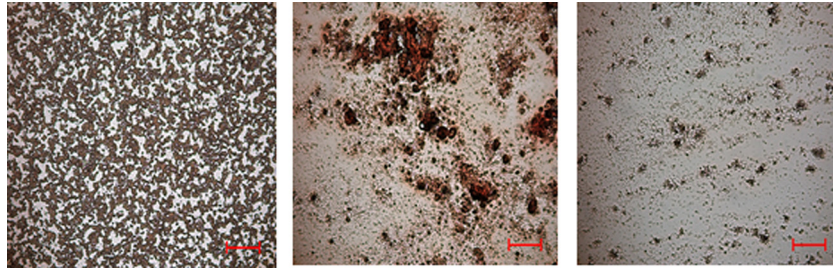


Fig. 10 Blood smears obtained from peripheral blood (left, as a reference) and CF device resin (middle and right) at the conclusion of the in vivo study. Microscopic examination revealed lack of evidence of clot or thrombosis in the CF device resin. Bar = 200 μm .

Significant Dox binding was noted with an 85%, 74%, and 83% decrease in relative preversus postfilter Dox concentrations at times 3, 10, and 30 min, respectively, after the initiation of Dox injection (Fig. 3(c)).

Discussion

A novel disposable endovascular catheter-based CF device was developed and successfully tested in vitro, with establishment of an in vivo large animal model for further evaluation. In vitro proof-of-concept was demonstrated with the first characterization of Dox binding to ion-exchange resins in a physiologic flow model in vitro and in blood in vivo. Prototypes were created of the CF device, a disposable temporarily positionable endovascular catheter-based device that could improve local and regional drug therapy during IAC. The device could be introduced via standard percutaneous central venous access and deployed in the veins of an organ undergoing IAC (such as the hepatic veins during hepatic IAC), in order to filter out drugs from the bloodstream using ion-exchange resins.

Flow studies demonstrated rapid high-capacity binding of Dox with a small volume (2.5 mL) of resin: after 10 min, 76% of the Dox within solution was captured. Moreover, during IAC simulation, the resin cartridge was able to filter out 95% of Dox in 45 min. Given that a 50 mg Dox infusion during IAC typically occurs over 10 min, and up to 50% (25 mg) of Dox passes directly through hepatic tumors into the systemic circulation via the hepatic veins, our studies demonstrate that the resin can capture on average 32 mg of Dox over 10 min. Interestingly, single pass studies demonstrated an average reduction of 50% of Dox concentration during each subsequent pass through the resin column with 99% of Dox removed after 6 passes. This efficiency is somewhat higher than the flow studies where the Dox solution recirculated through the resin column. The differences may potentially be due to concentration effects, as recirculation would lead to lower Dox concentrations and thus less efficient ion-exchange.

In porcine serum experiments, slower kinetics and binding capacity of the resin-Dox interaction was noted with 52% of Dox bound at 10 min compared to 76% in the PBS flow studies. A separate study demonstrated that these kinetic and binding capacity inefficiencies could be overcome by proportionally increasing the resin volume. These findings are concordant with the known pharmacokinetic profile of Dox, which has affinity for negatively charged serum albumin in the blood [29,30]. We are developing a full kinetic model to further elucidate interactions between Dox and albumin. These in vitro results ultimately provide the basis for the development of a CF device to potentially capture most of the escaping Dox during clinical IAC.

The CF1 device was successfully introduced via standard percutaneous central venous access and deployed in the suprahepatic IVC in vivo. While blood flow was occluded (Fig. 9), we suspect this was from stasis due to impedance from the catheter tip containing densely packed resin, and not due to poor resin

hemocompatibility. This was demonstrated by contrast venography performed 20 min after CF1 deployment, as well as IVC pressure measurements that revealed a significantly elevated pressure gradient of 20–30 mmHg (baseline 5–10 mmHg). Photomicrographs (Fig. 10) do not reveal thrombus among the resin in the device itself. These findings are consistent with the biocompatible characteristics of resin, which is highly sulfonated and composed of inert polystyrene. Subsequent studies are planned to better characterize pressure-flow dynamics in vivo with various catheter geometries and related cross sectional area occlusion.

The CF2 device was successfully introduced and deployed in the infrarenal IVC. The CF2 device was designed in order to avoid the immobilization of resin particles that led to high venous pressures and obstruction. A resin membrane was implemented to this aim with only partial obstruction of venous luminal cross sectional area. Compared to the CF1 device, there was less thrombosis noted, which was likely due to a smaller pressure gradient elevation (only 17 mmHg compared to 20–30 mmHg of the CF1 device). The experiment demonstrated significant Dox binding with an 85%, 74%, and 83% decrease in relative preversus postfilter Dox concentrations at times 3, 10, and 30 min, respectively after the start of Dox injection. Central and peripheral venous Dox concentrations were essentially undetectable by 30 min. This swine experiment demonstrates initial in vivo proof-of-concept of rapid high-capacity Dox filtration. Further studies must be performed with catheter designs that reduce venous obstruction. Moreover, these studies indicate that regardless of design, intravenous heparin may need to be administered or heparinization of the catheter itself may be needed to prevent thrombosis from blood stasis and the deployment of a relatively large intravascular foreign body over the course of at least 30 min.

Clinical series [5,7–13] studying the effects of chemofiltration via an extracorporeal dialysis-like system during hepatic IAC with Dox have demonstrated clinical proof-of-concept regarding the utility of this approach. Some instances have suggested that high-dose Dox therapy with such a dialysis-style filtration can induce long-term remission in patients with advanced HCC [10]. In certain cases, infusing a dose that was 4 \times higher than the Food & Drug Administration limit of lifetime Dox exposure, and would typically lead to life-threatening cardiac failure, did not lead to any cardiac toxicity. In these studies, systemic toxicities were significantly lowered due to reduction of the time of Dox exposure (area under the curve, (AUC)) over the course of a 90 min infusion, and yet tumor response was significant in patients. This indirectly suggests that high AUCs, which can be achieved from delivering high drug concentrations in short periods of time, may be key to tumor response. Moreover, response could be weighted toward higher drug concentrations rather than time-exposure based on prior studies suggesting tumors respond linearly to Dox concentration. The benefits of selective IAC compared to systemic IV Dox chemotherapy have been documented [6,31,32]. Nonetheless, IAC remains limited in terms of single and multisession dose delivery, since Dox has established lifetime dose limits (360 mg/

m²), above which the risk of irreversible heart failure rapidly climbs above 5%. On average, a patient with HCC receives 3–5 IAC procedures [6]; however, the CF device could confer a cost advantage since it could reduce the number of IAC procedures per patient by permitting delivery of a higher dose of chemotherapy in any given session. Although extracorporeal systems have demonstrated clinical proof-of-concept for high-dose Dox treatment in HCC, the complexities of extracorporeal devices have raised safety concerns [23]. A simple intravascular CF device could be safer, more easily deployed, and cost-effective.

Serum experiments confirmed the extraction of Dox seen in physiologic solutions with matching electrolyte molarity. It is important to note that the molar capacity of resin (0.6 meq monovalent cation/mL resin) is several orders smaller than the total body stores of electrolytes or plasma proteins. Thus, nonspecific binding to entities within circulating blood should be negligible. With the development of our swine model and preliminary promising in vivo filtration data, the efficacy and safety of the CF device in vivo will be further and more completely evaluated.

While cancer-free survival has improved over the past 20 yr for many patients with many malignancies, the increasingly recognized prevalence of cardiovascular disease in cancer survivors has been an unintended consequence of many cancer therapies, and threatens to offset improvements in cancer survival. The Centers for Medicare-Medicaid Services and Health Maintenance Organization databases within the United States indicate increased prevalence of billing codes for heart failure, myocardial infarction, and cardiac arrhythmias in patients treated for cancer [33–35]. Thus, there is an emerging need to develop cost-effective methods to eliminate antineoplastic drugs from systemic blood before they can cause cardiovascular damage or heart failure [36,37]. Moreover, cancer patients with baseline heart failure may have limited therapeutic options due to higher cardiac risk from even standard doses of Dox [38]. The CF device could potentially enable high-dose Dox treatments in patients regardless of cardiac risk as Dox would be eliminated from the bloodstream prior to reaching the heart.

Study Limitations

In vitro studies showed that gradients in pressure between proximal and distal sites of the CF1 device were 20–30 mmHg, suggesting that blood flow and hemodynamic characteristics through the device must be optimized since baseline central venous pressure is low (5–10 mmHg). A decrease in central venous pressure in vivo can lead to venous stasis, and ultimately vascular occlusion. Photomicrographs confirmed that occlusion of blood flow resulted from stasis due to resistance to blood flow at the CF1 device tip, and not from thrombosis in the resin itself. The proof-of-concept demonstrated by the CF2 device is only preliminary, as more animal studies will need to be performed to achieve statistical significance. The CF2 device led to some level of nonocclusive thrombus suggesting that further optimization of catheter design is necessary. Such thrombus could potentially change post-filter sample measurements by allowing for dilution from collateral or renal veins, which could lower postfilter concentrations. Additionally, in future in vivo experiments, animals or the CF device itself may be heparinized in order to prevent thrombosis. The combination of hepatic IAC with simultaneous CF device deployment and Dox filtration was not tested in this study, but are planned subsequently. Additional in vivo experiments using the established swine model are warranted to test advanced catheter designs with improved pressure-flow profiles based on ongoing benchtop and fluid-mechanical computer simulations.

Clinical Implications

HCC is the third leading cause of cancer death worldwide with hepatic IAC treatments being a mainstay of therapy for many patients. The CF device would enhance efficacy of hepatic IAC by reducing systemic Dox exposure and toxicity, and thereby

enable higher dose treatments, which could lead to improved clinical outcomes. Once in clinical use for HCC, the CF device could be used in patients with secondary liver tumors undergoing IAC, such as those patients with liver metastases from a number of malignancies. The CF device could also be adapted to treat nearly any solid organ tumor (kidney cancer, lung cancer, breast cancer, etc.), and a variation of the device could also be created for chemotherapeutics other than Dox.

The number of cancer survivors who experience subsequent cardiovascular events is large. In the US there are now over 13 million cancer survivors. For breast cancer survivors alone, it is estimated that \$800 million will be spent annually providing cardiovascular care [39,40]. Our proposed technique of CF may be translated into clinical setting for managing patients like these. In fact, specific CF devices could be also devised for an array of drugs with systemic toxicities (e.g., lytic agents) remote from their site of primary intended action, thus extending the CF technique beyond oncology.

Conclusion

A novel endovascular catheter-based CF device was developed and tested in vitro. A large animal model for further in vivo testing has also been established with promising preliminary data supporting rapid high-capacity Dox binding in vivo from blood. The CF device could serve as a platform technology for a new paradigm in drug therapy, enabling well-established, low-cost drugs to be used at higher doses, leading to less toxicity, and improved clinical outcomes.

Acknowledgment

This project was supported by:

- National Institutes of Health (NIH) and National Institute of Biomedical Imaging and Bioengineering (NIBIB) Grant Number 5T32EB001631
- NIH, National Center for Research Resources, and the National Center for Advancing Translational Sciences through the UCSF Clinical and Translational Science Institute (CTSI) Grant Number UL1 TR000004. Its contents are solely the responsibility of the authors and do not necessarily represent the official views of the NIH.
- Society of Interventional Radiology Foundation Resident Research Grant
- UCSF Department of Radiology Seed Grant
- UCSF Margulis Society Resident Research Grant

The work of Xi C. Chen and Nitash P. Balsara on the synthesis and characterization of the block copolymer membrane was supported by the Electron Microscopy of Soft Matter Program supported by the Office of Basic Energy Sciences, Materials Sciences and Engineering Division, U.S. Department of Energy under Contract No. DE-AC02-05CH11231.

References

- [1] Altekruse, S. F., McGlynn, K. A., and Reichman, M. E., 2009, "Hepatocellular Carcinoma Incidence, Mortality, and Survival Trends in the United States From 1975 to 2005," *J. Clin. Oncol.*, **27**(9), pp. 1485–1491.
- [2] Roche, A., Girish, B. V., de Baère, T., Baudin, E., Boige, V., Elias, D., Lasser, P., Schlumberger, M., and Ducreux, M., 2003, "Trans-Catheter Arterial Chemoembolization as First-Line Treatment for Hepatic Metastases From Endocrine Tumors," *Eur. Radiol.*, **13**(1), pp. 136–140.
- [3] Stuart, K., 2003, "Chemoembolization in the Management of Liver Tumors," *Oncologist*, **8**(5), pp. 425–437.
- [4] Llovet, J. M., Real, M. I., Montaña, X., Planas, R., Coll, S., Aponte, J., Ayuso, C., Sala, M., Muchart, J., Solà, R., Rodés, J., Bruix, J., and the Barcelona Liver Cancer Group, 2002, "Arterial Embolisation or Chemoembolisation Versus Symptomatic Treatment in Patients With Unresectable Hepatocellular Carcinoma: A Randomised Controlled Trial," *Lancet*, **359**(9319), pp. 1734–1739.
- [5] Hwu, W. J., Salem, R. R., Pollak, J., Rosenblatt, M., D'Andrea, E., Leffert, J. J., Faraone, S., Marsh, J. C., and Pizzorno, G., "A Clinical-Pharmacological Evaluation of Percutaneous Isolated Hepatic Infusion of Doxorubicin in Patients With Unresectable Liver Tumors," *Oncol. Res.*, **11**(11-12), pp. 529–537.

- [6] Buijs, M., Vossen, J. A., Frangakis, C., Hong, K., Georgiades, C. S., Chen, Y., Liapi, E., and Geschwind, J. F., 2008, "Nonresectable Hepatocellular Carcinoma: Long-Term Toxicity in Patients Treated With Transarterial Chemoembolization—Single-Center Experience," *Radiology*, **249**(1), pp. 346–354.
- [7] Curley, S. A., Newmann, R. A., Dougherty, T. B., Fuhrman, G. M., Stone, D. L., Mikolajek, J. A., Guercio, S., Kuroda, Y., Carrasco, C. H., and Kuo, M. T., 1994, "Complete Hepatic Venous Isolation and Extracorporeal Chemofiltration as Treatment for Human Hepatocellular Carcinoma: A Phase I Study," *Ann. Surg. Oncol.*, **1**(5), pp. 389–399.
- [8] August, D. A., Verma, N., Vaerten, M. A., Shah, R., Andrews, J. C., and Brenner, D. E., 1995, "Pharmacokinetic Evaluation of Percutaneous Hepatic Venous Isolation for Administration of Regional Chemotherapy," *Surg. Oncol.*, **4**(4), pp. 205–216.
- [9] Ku, Y., Tominaga, M., Iwasaki, T., Fukumoto, T., Muramatsu, S., Kusunoki, N., Sugimoto, T., Suzuki, Y., Kuroda, Y., and Saitoh, Y., 1998, "Efficacy of Repeated Percutaneous Isolated Liver Chemoperfusion in Local Control of Unresectable Hepatocellular Carcinoma," *Hepatogastroenterology*, **45**(24), pp. 1961–1965.
- [10] Ku, Y., Iwasaki, T., Fukumoto, T., Tominaga, M., Muramatsu, S., Kusunoki, N., Sugimoto, T., Suzuki, Y., Kuroda, Y., Saitoh, Y., Sako, M., Matsumoto, S., Hirota, S., and Obara, H., 1998, "Induction of Long-Term Remission in Advanced Hepatocellular Carcinoma With Percutaneous Isolated Liver Chemoperfusion," *Ann. Surg.*, **227**(4), pp. 519–526.
- [11] Ku, Y., Iwasaki, T., Fukumoto, T., Tominaga, M., Muramatsu, S., Kusunoki, N., Sugimoto, T., Suzuki, Y., Kuroda, Y., and Saitoh, Y., 1998, "Percutaneous Isolated Liver Chemoperfusion for Treatment of Unresectable Malignant Liver Tumors: Technique, Pharmacokinetics, Clinical Results," *Recent Results Cancer Res.*, **147**, pp. 67–82.
- [12] Ravikumar, T. S., Pizzorno, G., Bodden, W., Marsh, J., Strair, R., Pollack, J., Hendler, R., Hanna, J., and D'Andrea, E., 1994, "Percutaneous Hepatic Vein Isolation and High-Dose Hepatic Arterial Infusion Chemotherapy for Unresectable Liver Tumors," *J. Clin. Oncol.*, **12**(12), pp. 2723–2736.
- [13] Ku, Y., Tominaga, M., Iwasaki, T., Fukumoto, T., and Kuroda, Y., 2002, "Isolated Hepatic Perfusion Chemotherapy for Unresectable Malignant Hepatic Tumors," *Int. J. Clin. Oncol.*, **7**(2), pp. 82–90.
- [14] Porrata, L. F., and Adjei, A. A., 2001, "The Pharmacologic Basis of High Dose Chemotherapy With Haematopoietic Stem Cell Support for Solid Tumours," *Br. J. Cancer*, **85**, pp. 484–489.
- [15] Skipper, H. E., Schabel, F. M., Jr., Mellett, L. B., Montgomery, J. A., Wilkoff, L. J., Lloyd, H. H., and Brockman, R. W., 1970, "Implications of Biochemical, Cytokinetic, Pharmacologic, and Toxicologic Relationships in the Design of Optimal Therapeutic Schedules," *Cancer Chemother. Rep.*, **54**(6), pp. 431–450.
- [16] Walker, M. C., Parris, C. N., and Masters, J. R., 1987, "Differential Sensitivities of Human Testicular and Bladder Tumor Cell Lines to Chemotherapeutic Drugs," *J. Natl. Cancer Inst.*, **79**(2), pp. 213–216.
- [17] Doroshaw, J., 1996, "Anthracyclines and Anthracenediones," *Cancer Chemotherapy and Biotherapy*, 2nd ed., B. Chabner and D. Longo, eds., Lippincott-Raven, Philadelphia, pp. 409–434.
- [18] Winchester, J. F., Rahman, A., Tilstone, W. J., Kessler, A., Mortensen, L., Schreiner, G. E., and Schein, P. S., 1979, "Sorbenet Removal of Adriamycin In Vitro and In Vivo," *Cancer Treat Rep.*, **63**(11-12), pp. 1787–1793.
- [19] Sunil, B., Sutanjay, S., and Manjula, B., 2007, "Ion Exchange Resins in Drug Delivery," *Ion Exchange and Solvent Extraction*, CRC Press, Boca Raton, FL, pp. 103–150.
- [20] Lewis, A. L., 2009, "DC Bead: A Major Development in the Toolbox for the Interventional Oncologist," *Expert Rev. Med. Devices*, **6**(4), pp. 389–400.
- [21] Ku, Y., Fukumoto, T., Iwasaki, T., Tominaga, M., Samizo, M., Nishida, T., Kuroda, Y., Hirota, S., Sako, M., and Obara, H., 1995, "Clinical Pilot Study on High-Dose Intraarterial Chemotherapy With Direct Hemoperfusion Under Hepatic Venous Isolation in Patients With Advanced Hepatocellular Carcinoma," *Surgery*, **117**(5), pp. 510–519.
- [22] Pingpank, J. F., Libutti, S. K., Chang, R., Wood, B. J., Neeman, Z., Kam, A. W., Figg, W. D., Zhai, S., Beresneva, T., Seidel, G. D., and Alexander, H. R., 2005, "Phase I Study of Hepatic Arterial Melphalan Infusion and Hepatic Venous Hemofiltration Using Percutaneously Placed Catheters in Patients With Unresectable Hepatic Malignancies," *J. Clin. Oncol.*, **23**(15), pp. 3465–3474.
- [23] Dougherty, T. B., Mikolajek, J. A., and Curley, S. A., 1997, "Safe Anesthetic Management of Patients Undergoing a Novel Method of Treating Human Hepatocellular Cancer," *J. Clin. Anesth.*, **9**(3), pp. 220–227.
- [24] Satyapal, K. S., Rambiritch, V., and Pillai, G., 1995, "Morphometric Analysis of the Renal Veins," *Anat. Rec.*, **241**(2), pp. 268–272.
- [25] Siewiorek, G. M., Wholey, M. H., and Finol, E. A., 2007, "In Vitro Performance Assessment of Distal Protection Devices for Carotid Artery Stenting: Effect of Physiological Anatomy on Vascular Resistance," *J. Endovasc. Ther.*, **14**(5), pp. 712–724.
- [26] Weaver, M. E., Pantely, G. A., Bristow, J. D., and Ladley, H. D., 1986, "A Quantitative Study of the Anatomy and Distribution of Coronary Arteries in Swine in Comparison With Other Animals and Man," *Cardiovasc. Res.*, **20**(12), pp. 907–917.
- [27] Varga-Szemes, A., Kiss, P., Brott, B. C., Wang, D., Simor, T., and Elgavish, G. A., 2012, "Embozene Microspheres Induced Nonreperfused Myocardial Infarction in an Experimental Swine Model," *Catheterization Cardiovasc. Interv.*, **81**(4), pp. 689–697.
- [28] August, D. A., Verma, N., Andrews, J. C., Vaerten, M. A., and Brenner, D. E., 1994, "Hepatic Artery Infusion of Doxorubicin With Hepatic Venous Drug Extraction," *J. Surg. Res.*, **56**(6), pp. 611–619.
- [29] Chassany, O., Urien, S., Claudepierre, P., Bastian, G., and Tillement, J. P., 1996, "Comparative Serum Protein Binding of Anthracycline Derivatives," *Cancer Chemother. Pharmacol.*, **38**(6), pp. 571–573.
- [30] Ramanathan-Girish, S., and Boroujerdi, M., 2001, "Contradistinction Between Doxorubicin and Epirubicin: In-Vitro Interaction With Blood Components," *J. Pharm. Pharmacol.*, **53**(6), pp. 815–821.
- [31] Lai, C. L., Wu, P. C., Chan, G. C., Lok, A. S., and Lin, H. J., 1988, "Doxorubicin Versus no Antitumor Therapy in Inoperable Hepatocellular Carcinoma. A Prospective Randomized Trial," *Cancer*, **62**(3), pp. 479–483.
- [32] Simonetti, R. G., Liberati, A., Angiolini, C., and Pagliaro, L., 1997, "Treatment of Hepatocellular Carcinoma: A Systematic Review of Randomized Controlled Trials," *Ann. Oncol.*, **8**(2), pp. 117–136.
- [33] Bowles, E. J., Wellman, R., Feigelson, H. S., Onitilo, A. A., Freedman, A. N., Delate, T., Allen, L. A., Nekhlyudov, L., Goddard, K. A., Davis, R. L., Habel, L. A., Yood, M. U., McCarty, C., Magid, D. J., Wagner, E. H., and the Pharmacovigilance Study Team, 2012, "Risk of Heart Failure in Breast Cancer Patients After Anthracycline and Trastuzumab Treatment: A Retrospective Cohort Study," *J. Natl. Cancer Inst.*, **104**(17), pp. 1293–1305.
- [34] Hooning, M. J., Botma, A., Aleman, B. M., Baaijens, M. H., Bartelink, H., Kljin, J. G., Taylor, C. W., and van Leeuwen, F. E., 2007, "Long-Term Risk of Cardiovascular Disease in 10-Year Survivors of Breast Cancer," *J. Natl. Cancer Inst.*, **99**(5), pp. 365–375.
- [35] Patnaik, J. L., Byers, T., DiGiuseppe, C., Dabelea, D., and Denberg, T. D., 2011, "Cardiovascular Disease Competes With Breast Cancer as the Leading Cause of Death for Older Females Diagnosed With Breast Cancer: A Retrospective Cohort Study," *Breast Cancer Res.*, **13**(3), p. R64.
- [36] Travis, L. B., Rabkin, C. S., Brown, L. M., Allan, J. M., Alter, B. P., Ambrosone, C. B., Begg, C. B., Caporaso, N., Chanock, S., DeMichele, A., Figg, W. D., Gospodarowicz, M. K., Hall, E. J., Hisada, M., Inskip, P., Kleinerman, R., Little, J. B., Malkin, D., Ng, A. K., Offit, K., Pui, C. H., Robison, L. L., Rothman, N., Shields, P. G., Strong, L., Taniguchi, T., Tucker, M. A., and Greene, M. H., 2006, "Cancer Survivorship—Genetic Susceptibility and Second Primary Cancers: Research Strategies and Recommendations," *J. Natl. Cancer Inst.*, **98**(1), pp. 15–25.
- [37] Yeh, E. T. H., Tong, A. T., Lenihan, D. J., Yusuf, S. W., Swafford, J., Champion, C., Durand, J.-B., Gibbs, H., Zafarmand, A. A., and Ewer, M. S., 2004, "Cardiovascular Complications of Cancer Therapy: Diagnosis, Pathogenesis, and Management," *Circulation*, **109**(25), 3122–3131.
- [38] Schmitz, N., Kloess, M., Reiser, M., Berdel, W. E., Metzner, B., Dorken, B., Kneba, M., Trumper, L., Loeffler, M., 2006, "Four Versus Six Courses of a Dose-Escalated Cyclophosphamide, Doxorubicin, Vincristine, and Prednisone (CHOP) Regimen Plus Etoposide (MegaCHOEP) and Autologous Stem Cell Transplantation: Early Dose Intensity is Crucial in Treating Younger Patients With Poor Prognosis Aggressive Lymphoma," *Cancer*, **106**(1), pp. 136–145.
- [39] Brenner, H., 2002, "Long-Term Survival Rates of Cancer Patients Achieved by the End of the 20th Century: A Period Analysis," *Lancet*, **360**(9340), pp. 1131–1135.
- [40] Du, X. L., Fox, E. E., and Lai, D., 2008, "Competing Causes of Death for Women With Breast Cancer and Change Over Time From 1975 to 2003," *Am. J. Clin. Oncol.*, **31**(2), pp. 105–116.